Effect of Nonequilibrium Degree on Separation Factor in Carbon Isotope Separation by CO_2 Microwave Discharge

Masaaki Suzuki , Shinsuke Mori, Noritaka Matsumoto and Hiroshi Akatsuka*

Department of Chemical Engineering, Tokyo Institute of Technology
2-12-1 O-okayama, Meguro-ku, Tokyo 152-8552 Japan

Research Laboratory for Nuclear reactors, Tokyo Institute of Technology
2-12-1 O-okayama, Meguro-ku, Tokyo 152-8550 Japan

Abstract

In order to make the effect of nonequilibrium degree on the separation factor clear and avoid the lowering of separation factor due to the recombination reactions, the gas sampling was carried out at just behind the plasma region by using water-cooled gas sampling probe. In these experiments the local separation factor and the local nonequilibrium degree just behind the plasma region were obtained. The plasma gas compositions measured by the enthalpy probe system were substantially thermodynamic nonequilibrium conditions when the input energy was $4J/cm^3$. The measured maximum value of separation factor was 1.01, although it changes locally. In this paper we discuss about the measured separation factor and its nonequilibrium condition. Anyway, the only small value obtained in this experiments is similar to the recent data obtained by Kurchatov group [1] and is less than published data (1.20), which was measured spectroscopically [2].

I. Introduction

Electric discharge in some diatomic and triatomic gaseous molecules at the moderate pressures (10Torr < p < 200Torr) creates vibrationally nonequilibrium conditions. Since vibration-vibration transfer is faster than vibration-translation energy relaxation, average vibration energy is larger than gas temperature. High vibration energy can activate some endoergic chemical reactions, for example, nitrogen oxidation or dissociation of carbon dioxide. When the gas consists of two isotopic species, they have different populations in the higher vibration levels, since isotopic species of these gases have different vibrational quanta. This can lead to the different rate constants for some reactions activated by vibrations and isotope redistribution between reactants and products [3].

There were some experimental studies of isotope separation phenomena in the nonequilibrium electric discharge, such as silent discharge [4], impulse glow discharge [5] [6] [7], and D.C. glow discharge [8] for the past four decades. But first observation of isotope separation by using microwave discharge plasma was made by a group of P.N. Lebedev Institute in 1991 [2]. We started the study of carbon isotope separation by microwave discharge CO_2 plasma, stimulated by publications of that group, where nondissociated CO_2 after microwave discharge was enriched in ^{13}C with separation factor 1.20. This separation factor was measured by absorption spectroscopy of isotopic components of CO in the product gas. So one of our initial purposes of this study was to verify isotope separation by mass-spectroscopy of CO_2 and CO. But in our former works, such large separation factor could not be achieved [9]. Kurchatov group, Gorshunov et al. examined this isotope separation method too and reported that they also failed to reproduce high separation factor like Kerimkulov et al.

In microwave discharge plasma at a pressure of around 100 Torr, however, the plasma is apt to be heated thermally, not vibrationally and it is considerable that its plasma condition affects on the measured separation factor. In this study, in order to make its effect clear and avoid the lowering of separation factor due to the recombination reactions and isotope exchange reactions, the gas sampling was carried out at just behind the plasma region by using a sampling probe. In these experiments the local specific enthalpy, the local CO_2 conversion, and the local separation factor were obtained over the

range of axial distances from 10 mm to 50 mm downstream of the lower face of the waveguide and radial distances from 0 to 10.5 mm. By using these experimental data, we discuss the effect of nonequilibrium degree on separation factor.

II. Chemical Reaction Mechanism

In order to specify chemical reactions and chemical species in the CO_2 microwave plasma, the thermodynamic analysis was carried out. Figure 1 shows the thermal equilibrium compositions of CO_2 at 100Torr. In the temperature range below 5,000K, chemical species which exist in this system are CO_2, CO, O_2, and O and other species such as O_3 and C are negligible. Figure 1 also shows conversions for CO_2 and O_2. The conversion ratios for CO_2 and O_2 in the thermodynamic equilibrium are defined as follows

$$\beta = \frac{[CO]}{[CO]+[CO_2]} \tag{1}$$

$$\gamma = \frac{[O]}{[O]+2[O_2]} \tag{2}$$

β_{TEQ} and γ_{TEQ}, which are shown in Fig. 1, are the thermodynamic equilibrium value of the β and γ, respectively.

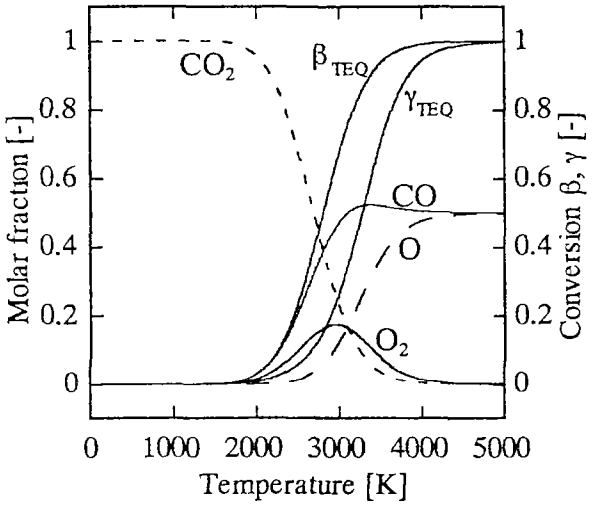

Fig. 1 Thermal equilibrium compositions and conversions

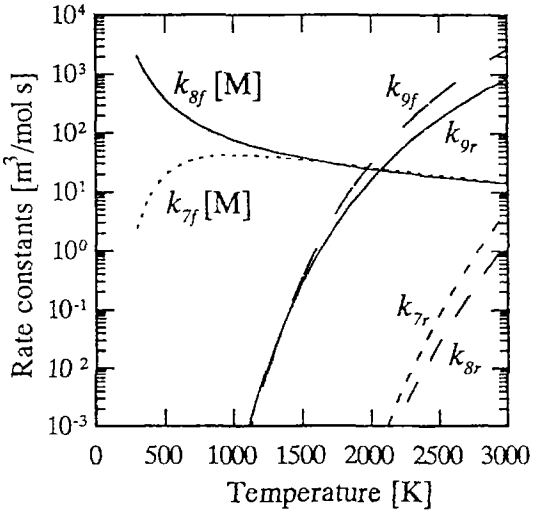

Fig. 2 Rate constants for forward and reverse reaction (7), (8), and (9). [M] is mole concentration of three-body particles.

1. Discharge Zone

In discharging plasmas of diatomic or triatomic gaseous molecules, it is well-known that it is possible to direct most of the electron energy into the molecular vibrational energy, by adjusting the reduced electric field E/N into the range of $(2 - 6)\times 10^{-16}$V·cm^2 [10].

Under such conditions, the quantum states of the vibrational modes are populated in a markedly non-Boltzmann distribution: the higher vibrational energy states are overpopulated with respect to the lower energy ones. This is because the rate of intermolecular vibration-vibration exchange (V-V) is higher than transfer of vibration energy into translational one (V-T) and the energy spacing of the higher states is smaller than that of the lower ones due to the anharmonicity of the molecular vibrations. This can lead to the high rate constants of vibrationally excited chemical reactions.

$$CO_2(v) + CO_2(v') \rightarrow CO + O + CO_2 \tag{3}$$

Since isotopic species of CO_2 gas have different vibrational quanta, they can have different vibrational distribution. It can result in the different rate constants of endothermic reactions, therefore the isotopic species will be redistributed between the reactants and the products.

There can be some other possible channels of dissociation: through the direct excitation by an electron impact

$$CO_2 + e \rightarrow CO + O + e \quad (4)$$

or the thermal decomposition

$$CO_2 + M \rightarrow CO + O + M \quad (5)$$

Dissociation through direct electron impact (4) seems to be isotopically nonselective and thermal decomposition (5) is surely isotopically nonselective, so it is important for high separation factor to enhance the reaction (3) and quench the reaction (4) and (5), adjusting the discharge conditions.

The most probable final stage of CO_2 decomposition is as follows:

$$CO_2(v) + O \rightarrow CO + O_2 \quad (6)$$

This reaction seems to be isotopically nonselective or can have an opposite effect to (3) because activation energy of this reaction is relatively low as compared with (3). Through these reaction channels, CO_2 decomposes and there can exist chemical species CO_2, CO, O_2, and O at the entrance of recombination zone. It depends on the discharge conditions which channel is dominant.

2. Recombination Zone

In the recombination zone, recombination reactions of atomic oxygen, as listed below, are dominant.

$$CO + O + M \rightarrow CO_2 + M \quad (7)$$

$$O + O + M \rightarrow O_2 + M \quad (8)$$

If the chemical species have high translational energy or are excited vibrationally, following reactions can be competitive with three-body reactions (7) and (8).

$$CO_2 + O \rightarrow CO + O_2 \quad (9)$$

$$CO + O_2 \rightarrow CO_2 + O \quad (10)$$

Rate constants for these reactions and their reverse reactions are represented in Fig. 2 as a parameter of gas temperature. Reactions (7), (9), and (10) can lead to the carbon isotope redistribution between CO_2 and CO (these reactions are isotopically nonselective). However, we can see from Fig. 2 that, in the temperature range < 500K, the three-body recombination of atomic oxygen (8) are dominant and other reactions are negligible. In the probe gas line, sampling gas is cooled down to the room temperature rapidly. So it seems reasonable to suppose that the only reaction which occurs in the probe gas line is the three-body recombination of atomic oxygen (8).

Table 1 Chemical reaction and rate constants in the recombination zone [11]

	Reaction	Rate constant
(R1)	$CO + O + M \rightleftharpoons CO_2 + M$	$k_{1f} = 1.0 \times 10^7 T^{-1.5} \exp(-20900/RT)$
(R2)	$O + O + M \rightleftharpoons O_2 + M$	$k_{2f} = 1.9 \times 10 \exp(7480/RT)$
(R3)	$CO_2 + O \rightleftharpoons CO + O_2$	$k_{3b} = 2.5 \times 10^6 \exp(-199390/RT)$

In the case of large CO_2 conversion, in addition, in is necessary to take into account possible CO_2 - CO isotope exchange reactions:

$$^{12}CO_2 + {}^{13}CO \rightleftharpoons {}^{12}CO + {}^{13}CO_2 \qquad (11)$$

This reaction also leads to the carbon isotope redistribution between CO_2 and CO. Of course, rate constants for forward and reverse reactions are small at room temperature. But under the conditions of nicrowave discharge, these isotope exchange reactions may be competitive with those of CO_2 dissociation reactions and equilibrium constant for reaction (11) is not clear because both reactions are activated by CO_2 and CO vibrations.

III. Experimental Set-up and Procedure

A schematic of the experimental apparatus is shown in Fig.3. The microwave generator was operated at the frequency 2.45GHz. Its output power was up to 4.9kW. The microwave was fed through rectangular waveguide with a cross section of $110 \times 55 mm^2$. The plasma chemical reactor was made of a quartz tube with an inner diameter 26mm, crossing the waveguide perpendicularly to its wide side. At the quartz tube entrance, there is gas distributor which makes gas flow rotate and so creates the partial thermal isolation of quartz walls from hot plasma and stabilized discharge near the center of tube.

Inside the quartz tube, a water-cooled gas sampling probe is equipped (Fig.4). The schematic diagram of the gas sampling probe is shown in Fig. 5. The probe employed has an outer diameter of 4 78 mm and inner diameter of 1.27 mm. It is constructed from three concentric thin wall stainless steel tubes. The median tube guides the cooling water to and from the tip of the probe. Through the inner tube, the samples of the gas mixture are drawn out of the plasma reactor and the specific enthalpy of the sampling gas is measured by the enthalpy probe system.

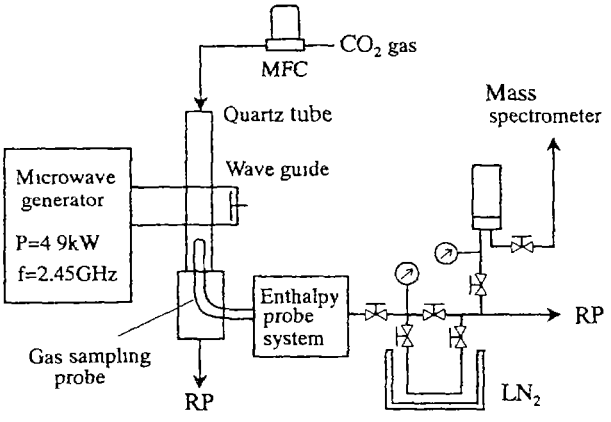

Fig. 3 Schematic diagram of the experimental set-up

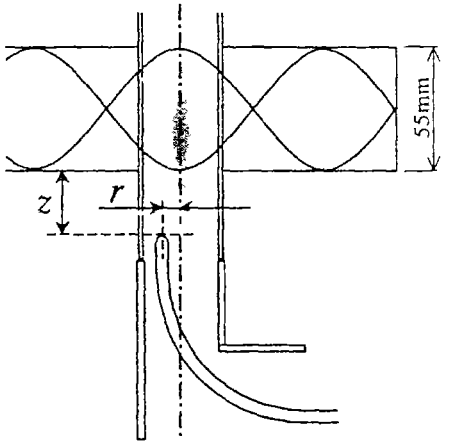

Fig. 4 Schematic diagram of the sampling probe location

The enthalpy probe system, which gives the specific enthalpy of sampling gas from the temperature rise of the cooling water, includes a water-cooled sampling probe, a closed loop cooling water recirculation system, and a gas sampling line which consists of a mass flow controller, pressure gauge, and a vacuum pump [12]. The measurement is based on a two-step energy balance on the cooling water circulating in the enthalpy probe. The first is a "tare" measurement of the heat load on the probe in the absence of gas sampling, i.e. "no-flow" case. The second is a measurement of the heat load under "sampling" conditions, when a known amount of gas is extracted from the plasma. The difference between the heat load on the probe cooling circuit in these two cases represents the energy associated with the extracted gas sample. The specific enthalpy of the gas at the sampling point can be calculated

using the following equation:

$$\dot{m}_g (h_{in} - h_{out}) = m_w C_{pw} (\Delta T_{sampling} - \Delta T_{tare}) \quad (11)$$

where h_{in} and h_{out} are the specific enthalpy at the probe inlet and outlet respectively, $\dot{m}_w$ and $\dot{m}_g$ are the mass flow rates of the cooling water and the gas sample respectively, C_p is the specific heat of cooling water and ΔT is the cooling water temperature rise.

After leaving the enthalpy probe system, the samples of the gas mixture were analyzed by mass-spectrometer during discharge or after to determine CO_2 conversion and carbon isotope contents in CO_2 or CO. The conversion of CO_2 was also measured by CO_2 partial pressure after discharge (CO_2 was frozen by LN_2, then CO + O_2 pumped.).

Experimental conditions were set in the same conditions as Kerimkulov et al. did (The maximum separation factor 1.20 was obtained with input energy 7J/cm^3). The CO_2 flow was regulated by a flow-meter within the range of 0.1-0.4Nl/s. The power absorbed by the plasma was 1-2kW, and the discharge pressure was regulated within 50 - 150 Torr by change of the pumping rate.

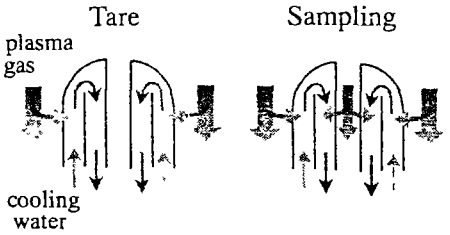

Fig. 5 Schematic diagram of the enthalpy probe

IV. Results and Discussion

In this section, first, the local gas temperatures are estimated from the specific enthalpy; besides, the thermodynamic equilibrium conversions are derived from those gas temperatures thermodynamically. Then nonequilibrium degree is evaluated, comparing thermal equilibrium conversion with measured conversion. After that, local separation factor is compared with nonequilibrium degree.

1. Local value of the CO_2 conversion and specific enthalpy

The spatial distribution of the dissociation degree and the specific enthalpy, which were measured by the above mentioned probe system, are shown in Figs. 6 and 7, respectively. Unfortunately, the local measurements shown in these figures could not be extended to the area (z, r) = (10, 0), (10, 2), and (10, 4) with input energy 8J/cm^3 because of thermal damage of probe due to its overheating. Both the local CO_2 conversion and the local specific enthalpy are very high in the central-upstream part and show the steep axial and radial gradient over the whole sampling area.

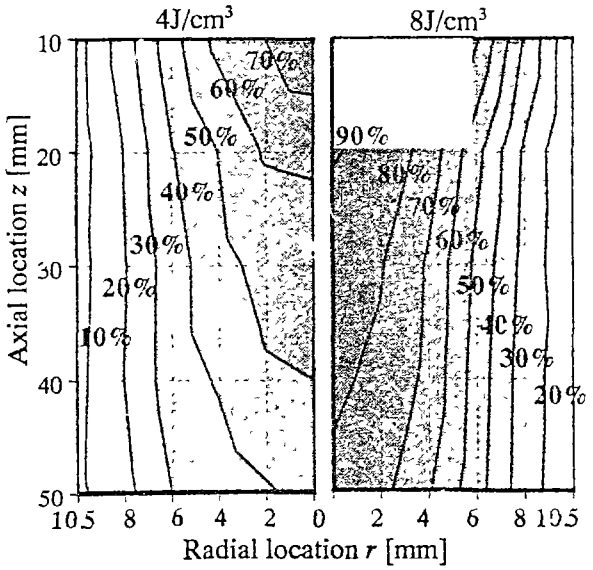

Fig. 6 The spatial distribution of the CO_2 conversion with input energy E_{in} = 4J/cm^3 and 8J/cm^3

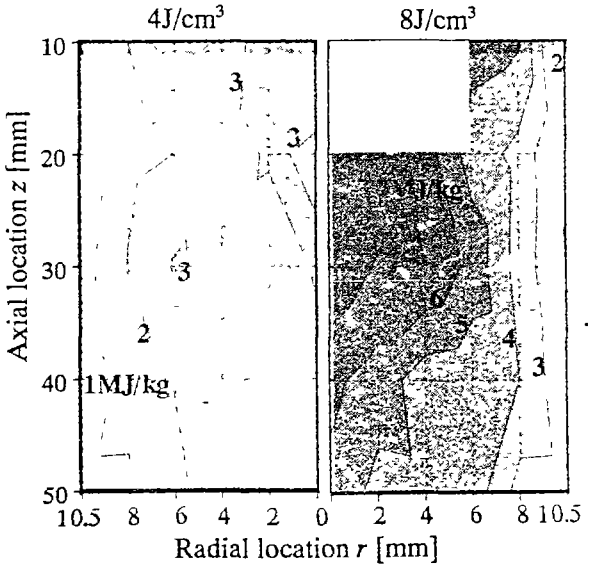

Fig. 7 The spatial distribution of the specific enthalpy with input energy E_{in} = 4J/cm^3 and 8J/cm^3

2. Estimation of the local gas temperature from specific enthalpy

The local gas temperatures were estimated from the specific enthalpy of sampling gas. As the chemical reactions take place in the probe gas line, the specific enthalpy measured by enthalpy probe system includes not only kinetic energy of sampling gas but also reaction enthalpy. So specifying the chemical composition is indispensable to determine the gas temperature. As mentioned above, three-body recombination reaction of atomic oxygen would occur in the probe gas line.

$$O + O + M \rightarrow O_2 + M \tag{8}$$

So it is necessary to know the concentration of atomic oxygen at the probe inlet, but it is impossible to measure it. If x_O is the molar fraction of the atomic oxygen at the probe inlet, the gas temperature T_g at the probe inlet can be given by

$$M_{mix}(h_{in} - h_{out}) = \int_{T_{out}}^{T_g} C_{p\,mix}\,dT - \frac{1}{2}\Delta h_{(8)} x_O \tag{13}$$

$$M_{mix}(T) = \sum_i M_i x_i \tag{14}$$

$$C_{p\,mix}(T) = \sum_i C_{p_i} h_i x_i \tag{15}$$

where $h_{(8)}$ is the reaction enthalpy of the reaction (8), h_{in} and h_{out} are the specific enthalpy at the probe inlet and outlet respectively, $C_{p\,i}$ and $C_{p\,mix}$ are the specific heat of chemical species i and the mixture respectively, M_i and M_{mix} are the atomic mass of chemical species i and the mixture respectively, x_i is the molar fraction of chemical species i, and T_{out} is the gas temperature at the probe outlet. When the reactant is pure CO_2 and products are CO_2, CO, O_2, and O, there is a relationship between x_O, β and γ as follows:

$$x_O = \frac{2\beta\gamma}{2 + \beta + \beta\gamma} \tag{16}$$

Finally, the local gas temperature T_g can be expressed as the function of the local specific enthalpy h_{in}, the local CO_2 conversion ratioβ, and the local O_2 conversion ratioγ:

$$T = f(h_{in}, \beta, \gamma) \tag{17}$$

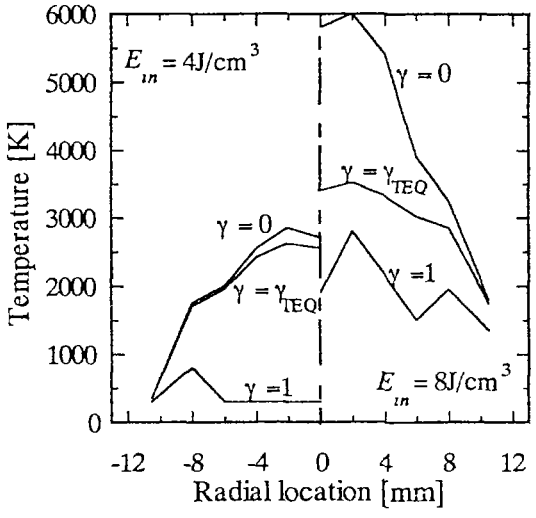

Fig. 8 Radial profile of gas temperature at an axial location 20mm downstream of the lower face of the waveguide with input energy E_{in} = 4J/cm^3 and 8J/cm^3.

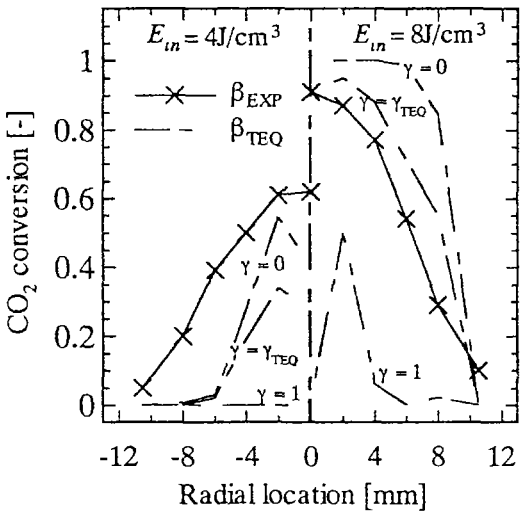

Fig. 9 Radial profile of CO_2 conversion at an axial location 20mm downstream of the lower face of the waveguide with input energy E_{in} = 4J/cm^3 and 8J/cm^3.

The local specific enthalpy and the local CO_2 conversion ratio can be determined by experiments but the local conversion ratio of O_2 molecules are unknown, so the local gas temperatures are determined as a parameter of O_2 conversion ratio, $0< \gamma <1$. Figure 8 shows the radial profiles of the calculated temperature for $\gamma = 0$, 1, and γ_{TEQ} at an axial location of 20mm downstream of the lower face of the waveguide. We can see from this figure that the local gas temperatures can not be determined specifically and have the wide range due to the γ. In the case of the input energy 8J/cm^3, however, it is clear that for all the value of γ, the local gas temperatures are too high to quench the thermal CO_2 decomposition (5).

3. Deviation of measured composition from the local thermodynamic equilibrium composition

If the thermal decomposition of CO_2 were to be dominant, the chemical composition of the plasma gas would become close to thermal equilibrium. In that conditions, isotope separation phenomena would not be performed since thermal decomposition is surely isotopically nonselective. If the chemical composition of plasma gas are in thermodynamic nonequilibrium, thermal decomposition is not be dominant and other channels of CO_2 dissociation can control the field. So it is interesting to evaluate the nonequilibrium degree of microwave plasma locally by comparing the local thermodynamic equilibrium conversion of CO_2 derived from the specific enthalpy with the measured local CO_2 conversions. Fig. 9 shows the radial profiles of the estimated local CO_2 conversion for $\gamma = 0$, 1, and γ_{TEQ} and measured local CO_2 conversion at an axial location of 20mm downstream of the lower face of the waveguide. The local thermodynamic equilibrium conversion ratios of CO_2 have some range due to the ambiguity of the local gas temperature estimated from the local specific enthalpy. But, even though the γ would be 0, the measured local conversions of CO_2, β_{EXP}, with the input energy 4J/cm^3 are larger than those calculated thermodynamically from the local specific enthalpy and this represents the nonequilibrium states of plasma.

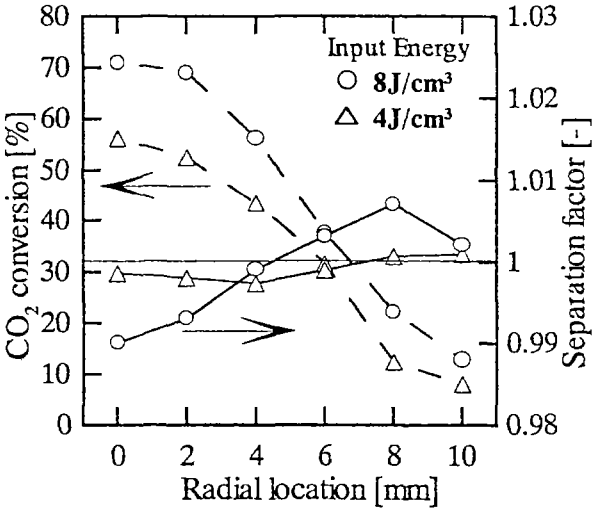

Fig. 10 Radial profile of separation factor and CO_2 conversion

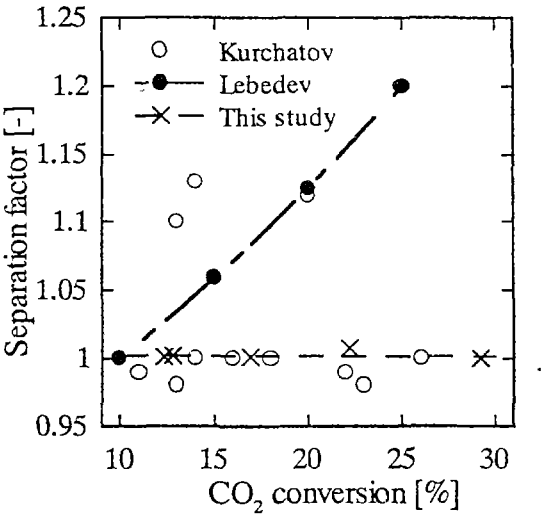

Fig. 11 Experimental results of separation factor

4. Effects of nonequilibrium degree on local separation factor

As mentioned above, when the dissociation through vibration excitation are dominant over other dissociation channels, high separation factor would be expected. It means that nonequilibrium degree is surely not irrelevant to the isotopic selectivity. So it is important to note the relationship between the local nonequilibrium degree and the local isotope separation factor. In this study, separation factor α is defined as follows.

$$\alpha = \frac{\left([^{13}CO_2]/[^{12}CO_2]\right)_{product}}{\left([^{13}CO_2]/[^{12}CO_2]\right)_{reactant}} \tag{18}$$

This separation factors together with CO_2 conversion β at an axial location of 20mm downstream of the lower face of the waveguide are shown in Fig. 10. We can see from this figure that in the central area of the radial direction ($r \simeq 0$) CO_2 was depleted in ^{13}C and in the middle area of the radial direction ($r \simeq 8$) CO_2 was enriched in ^{13}C, slightly. High separation factor was expected in the case of input energy 4J/cm^3, but practically, separation factor was very small ($0.99< \alpha <1.01$) with any experimental condisions.

5. Comparison of our results with other studies

Since the gas sampling process by water-cooled probe makes it possible to avoid the lowering of separation factor due to the recombination reactions and isotope exchange reactions, high separation factor was expected in this study compare to previous results. However, we could not get such high separation factor (1.20) as reported by Kerimkulov et al. Kurchatov group, Gorshunov et al. also reported that they failed to reproduce high separation factor like Kerimkulov et al. as shown in Fig.11 Although it was mentioned by Gorshunov et al. that results of Kerimkulov et al. may include some error, there still remained a doubt of the lowering of separation factor due to the chemical reaction in the recombination zone. Our experiments has extinguished this doubt completely and we can agree with Gorshunov et al. Therefore, we can guess with certainty that the results of Kerimkulov et al. has some error.

V. Conclusion

In order to make the effect of nonequilibrium degree on the separation factor clear and avoid the lowering of separation factor, the gas sampling was carried out at just behind the plasma region by using water-cooled gas sampling probe and measurements of the specific enthalpy, CO_2 conversion, and separation factor were performed locally. The following conclusions were obtained from the results and discussion.

(1) Both the local CO_2 conversion and the local specific enthalpy are very high in the central-upstream part and show the steep axial and radial gradient over the whole sampling area.

(2) The local gas temperatures and the local thermodynamic equilibrium CO_2 conversions were obtained from the local specific enthalpy as a parameter of O_2 conversion ratio at the sampling point. In the case of the input energy 8J/cm^3, however, it is clear that for all the value of γ, the local gas temperatures are too high to quench the thermal CO_2 decomposition. And, in the case of the input energy 4J/cm^3, The plasma gas compositions measured by the probe system were substantially thermodynamic nonequilibrium conditions to any γ.

(3) The local value of separation factor changed locally, but practically those value were very small ($0.99< \alpha <1.01$). We could not get such high separation factor (1.20) as reported by Kerimkulov et al. This result agrees with that of Gorshunov et al.

References

[1] N. M. Gorshunov et al., Abstracts of 3rd All-Russian Sci. Conf. "Phys. Chem. Processes at Selection of Atoms and Molec.", 33 (1998).

[2] Kerimkulov M. A. et al., JETP Lett. **54**, 208 (1991).

[3] E. Ploenjes, I. Adamovich, V.V. Subramaniam, and J.W. Rich, AIAA Paper 98-0993, Jan (1998).

[4] I.A. Semiokhin, G.M. Panchenkov, V.K. Korovkin and A.V. Borisov, Russ. J. Phys. Chem. **33**, 226 (1959).

[5] T.J. Manuccia and M.D. Clark, Appl. Phys. Lett. **28**, 372 (1976).
[6] N.G. Basov, E.M. Belenov, L.K. Gavrilina, V.A. Isakov, E.P. Markin, A.N. Oraevskii, V.I. Romanenko, and N.B. Ferapontov, JETP Lett. **19**, 190 (1974).
[7] T.G. Abzianidze, A.B. Andryushchenko, A.B.Bakhtadze, A.S. Elizarov and G.I. Tkeshelashvili, *Stable Isotopes in the Life Sciences* (IAEA, Vienna), 69 (1977).
[8] R. Farrenq, C. Rossetti, G.Guelachvili and W. Urban, Chem. Phys. **92**, 389 (1985).
[9] A.N. Ezoubtchenko, C. Nagaoka, H. Akatsuka and M. Suzuki, *Abstracts of 1997 Fall Meeting of the Atomic Energy Society of Japan,* L68, 970 (1997) (in Japanese).
[10] W.L. Nighan, Phys. Rev. A **2**, 1989 (1970).
[11] Y. Mori et al., *Formation Mechanisms and Controls of Pollutants in Combustion System*, Japan Society of Mechanical Engineers, (1980) (in Japanese).
[12] M. Rahmane, G. Soucy and M.I. Boulos, Rev. Sci Instrum. **66**, 3424 (1995)